

COB-2023-0728

LOW COST PELTIER MODULES IN EVALUATION OF PRISMATIC LITHIUM-ION CELLS THERMAL BEHAVIOR

Luciano Amaury dos Santos

Joaquim Manoel Gonçalves

Samuel Luna de Abreu

Andre Luiz Fuerback

Daniel Godoy Costa

Adriano de Andrade Bresolin

Instituto Federal de Santa Catarina, Av. Mauro Ramos, 950 – Centro -CEP 88020-300 – Florianópolis - SC

luciano.santos@ifsc.edu.br, joaquimm@ifsc.edu.br, abreu@ifsc.edu.br, andre.fuerback@ifsc.edu.br, danielgodoy@ifsc.edu.br,

adriano.bresolin@ifsc.edu.br

Abstract. *Lithium-ion batteries have been used for an extensive range of quite demanding applications, and are supplied in a large variety of shapes and sizes by many manufacturers around the world. The electro-thermal-chemical characterization of the batteries electro-chemical cells is receiving attention, but the variety of these cells is such that frequently the end users need to make some characterization themselves. The most usual and standardized approach is to make controlled cell charges and discharges in an environment of more or less controlled temperature, without control of the heat released and absorbed by the cell along these processes. Another pretty common approach is to use an adiabatic calorimeter to measure the heat released by the battery, without temperature control. This work presents initial results of an effort to develop a very low cost Arduino based equipment to control a prismatic cell surface temperature, with the future intention of monitoring the heat it releases, using Peltier modules. The influence of the ambient temperature was minimized using expanded polystyrene plates. The use of a heat conduction analytical solution in thermophysical properties estimation employing the equipment here presented is exemplified. The already performed experiments revealed some cautions to be exerted in the use of such low cost equipment: a temperature set-point below the environment dew point caused some trouble, the electromagnetic noise produced by switched power supplies was really detrimental to temperature measurements performed using analog sensors. In spite of these difficulties, these tests indicated that the temperature control by low cost Peltier modules can be very effective and practical in prismatic Li-ion cells characterization experiments.*

Keywords: *characterization, Li-ion cells, Peltier modules*

1. INTRODUCTION

Some use of Peltier modules as an alternative to conventional liquid and air cooling strategies, for little packages of small cylindrical Li-ion battery cells is reported in the literature (Li *et al.*, 2019; Lyu *et al.*, 2021; Singh *et al.*, 2021). The low coefficient of performance, COP, (under sizeable temperature difference and heat flux) of these Peltier modules, however, have hindered its use in larger scale. For laboratory setups, used for short periods of time, the low COP is not so problematic and the possibility of very effective temperature control allowed by the Peltier modules is rather conducive. Aware of this the authors aimed to develop a laboratory application of Peltier modules helpful in the characterization of a prismatic relatively large (1.8 kg, 113 A·h) NMC(881)/graphite Li-ion cell model CALB L221N113A.

The authors first assessment of the mentioned Li-ion cell thermal properties, for use in previous works (Gonçalves *et al.*, 2022; Santos *et al.*, 2022), was made using ice and water baths. This approach was subsequently avoided due to difficulties in isolating the cell from water while keeping good thermal contact and allowing passage of the temperature sensors wires, the fire risks associated to the eventual contact of metallic lithium with water and the corrosion of the cell electrical terminals promoted by moisture. These risks made clear that an alternative mean of performing such properties assessments should be devised and the use of low cost Peltier modules (available at refrigeration shops for use in silent domestic drinking fountains) seemed to be a promising one.

1.1 Specific goals

The primary goal at the start of the present work was to put together a low cost equipment able to safely drive a prismatic Li-ion cell to a chosen temperature (between -20 and 55 °C to avoid any cell damage) and keep it at the chosen temperature.

A secondary goal was to verify the viability of using this equipment directly to assess some thermal properties of the cell and get some experience in using Peltier modules for this kind of task. The work of Muratori *et al.* (2010) indicated that good results could be achieved, but it should be noted that the commercial cold plate coolers used by them are not so inexpensive as the Peltier modules to be used here and that the Li-ion cell tested by them was much smaller than the considered here and was just 7,2 mm thin. An essential tool for achieving this secondary goal is a mathematical model like that described in section 4.

There are more conventional and reliable ways of assessing thermal properties of a battery cell (Liu and Lijun, 2021; Murashko *et al.*, 2020; Maleki *et al.*, 1999) but the equipment required was not as readily available to the authors as the material used in the assembly described in section 2.

1.2 Essential information about the Peltier modules

The Physics behind Peltier modules are explained in sources like Thermoelectric Cooling (2023) and will not be reviewed here. Nevertheless it is convenient to recall some practical facts about these components. A Peltier module is generally a thin plate (the model used in the present work had ceramic external surfaces) with two wires protruding from its sides to connected it to a DC power supply. When it is powered a heat flow is created from one of its sides to the other (which side is cooled and which is heated may be reversed changing the polarity of the connections to the power supply). The heated side receives all the heat drawn from the cooled side plus some heat internally generated (the module has its own inefficiency as the second law of thermodynamics remains valid). A consequence of this greater ability of Peltier modules to heat than to cool is the fact that, if adequate heat dissipation means (as a heat sink) are not provided at the heated side, it easily gets overheated and permanently damaged (since its internal semiconductor - bismuth telluride mostly - elements do not endure temperatures above 200 °C). Another aspect to be remembered when using the Peltier module as a cooling device is that its performance is inferior to that of a vapor compression system (Hermes and Barbosa, 2012).

The performance of a Peltier module is described in charts provided by its manufacturers (the performances of modules of different manufacturers hardly present any difference if the modules have the same dimensions, materials, number of couples and capacity). For the model used in the present work a pretty accurate chart is offered by TE Technology (2013). Computer implementations of mathematical models for the Peltier module performance are readily available, one of those is used as example in Mathworks (2023), but they were not explored in the present work.

2. EXPERIMENTAL APPARATUS

The temperature control system was composed of:

- two Peltier thermoelectric modules TEC1-12708 thermally coupled to heat sinks;
- a 12 V switched voltage supply (adjustable between 11,5 and 13,2 V) and 30 A capacity to power the Peltier modules;
- an Arduino MEGA 2560 controller board with an LCD Keypad Shield (to provide a portable HMI);
- a driver BTS7960 in H bridge to realize the pulse width modulation (PWM) of the power delivered to the Peltier modules and the polarity change when commuting from heating to cooling and vice versa;
- a Pt100 thermoresistor connected to a Bigeng BIG 1608-2 signal conditioning board (this Pt100 is the sensor used to control the Peltier modules);
- another 12 V voltage source (typical of a portable personal computer) to power the controller board and the thermoresistor signal conditioner (without the much higher noise of the 30 A power supply used for the Peltier modules);
- an LM35 temperature sensor used to monitor the temperature at the Li-ion cell side opposite to that where the Peltier modules were coupled.

Many researchers have used, for different purposes, systems with some resemblance to this one, a well documented example is presented by Cunha (2019). The control method adopted in the present work was of the proportional-integral (PI) type, with constants $K_P = 50$ and $K_I = 0.5$ chosen following the section 10.5 of the book written by Normey-Rico and Morato (2021). The PID library written for Arduino by Beauregard (2017) was used. This system (except the Peltier modules and the sensors to be attached to the Li-ion cell) is shown in Fig. 1. Eventually the switched voltage source was replaced by an adjustable (from 0 to 30 V and 0 to 10 A) linear power supply .

To clarify how the temperature sensors, the Peltier modules and the insulation were assembled around the Li-ion cell the sequence of pictures shown in Fig. 2 was created. Figure 2(a) shows the LM35 temperature sensor above the bottom expanded polystyrene thermal insulation plate. Figure 2(b) shows the Li-ion cell placed above the LM35 sensor.

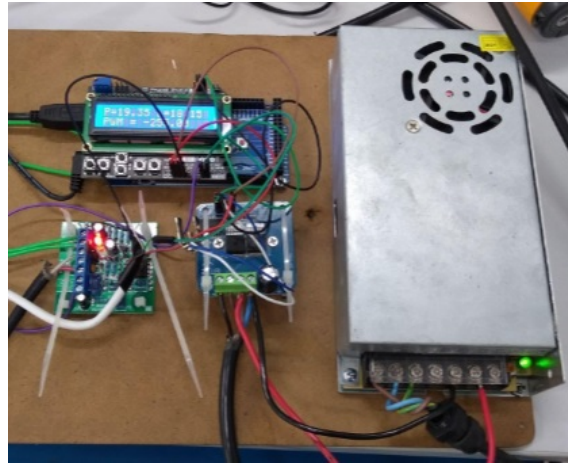


Figure 1. Temperature control electronics.

Figure 2(c) shows all the expanded polystyrene insulation already in its place around the Li-ion cell, but the sandwiches composed by the Peltier modules between the heat sinks and small aluminum plates are upside-down and aside from their final positions. Figure 2(d) shows the assembly complete, with the Peltier module sandwiches already at their intended places. White thermal grease (visible in Figs. 2(b) and (c)) was applied at the interfaces between the LM35 sensor and the cell, inside the Peltier module sandwiches and between these sandwiches and the cell.

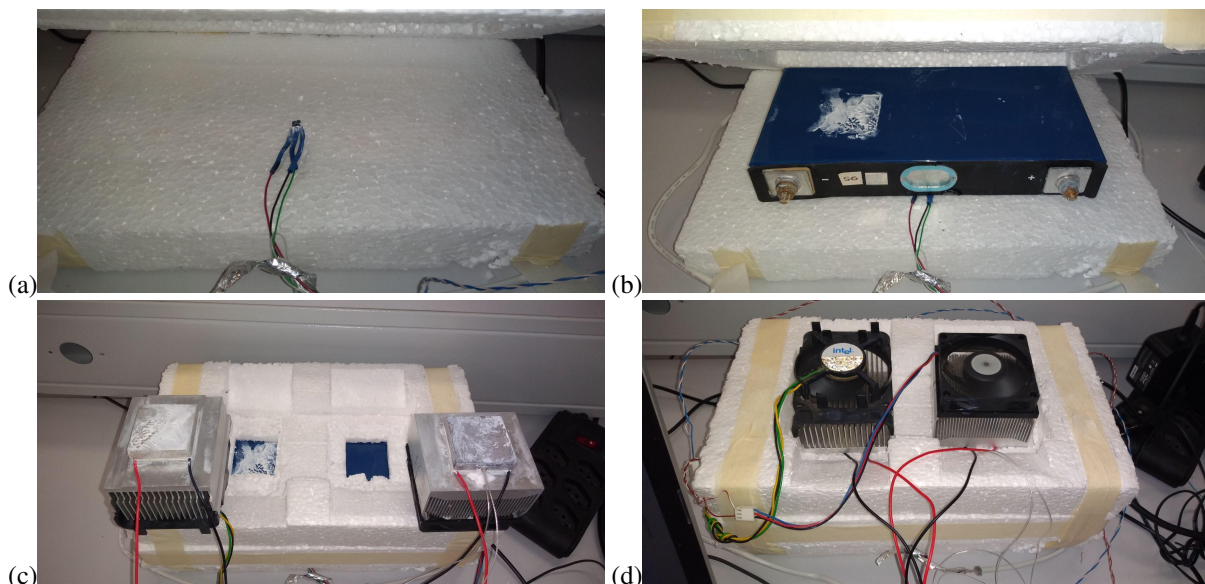


Figure 2. Assembly of sensors, Peltier modules and insulation around the Li-ion cell.

The role of the Peltier modules and of the heat sinks (acting as sinks of cold when the Li-ion cell is heated) are easy to grasp, but the small (40 x 40 x 10 mm) aluminum plates in the sandwich deserve explanation. The one appearing at the left side of the pictures in Fig. 2 has the Pt100 temperature sensor inside a cylindrical hole drilled in that plate (to avoid difficulties in thermally coupling the Pt100 cylindrical encapsulation with the Peltier module and with the Li-ion cell). The other is used to make the assembly nearly symmetrical. Both these small plates work as spacers providing, with the Peltier modules, room for a 12 mm layer of expanded polystyrene thermal insulation between the heat sinks extensions beyond the Peltier module size and the Li-ion cell.

Figure 3 shows the complete apparatus including a personal computer to receive the data sent via USB cable by the Arduino and also the adjustable linear source used eventually used (in one test with Peltier modules under 8.5 V and other under 12 V and improved cooling).

3. EXPERIMENTAL RESULTS

The intention in the experiments here presented was to impose a step change to the temperature at the Li-ion cell side where the Peltier modules were coupled and monitor the temperature response at the opposite side of the cell. A series of

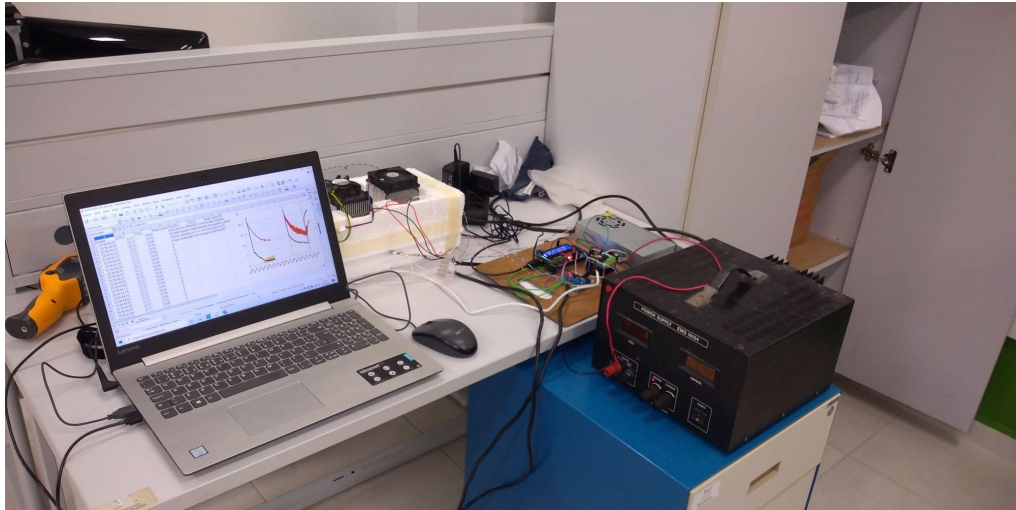


Figure 3. The complete experimental apparatus performing data acquisition and using an adjustable linear power supply.

tests was performed, applying different voltage levels to the Peltier modules (with the switched power supply one could obtain or 12 V, connecting them in parallel, or 6 V, with them in series, but using the adjustable linear power supply almost any value between 0 and 12 V could be chosen).

3.1 The best results

In some tests the control system goal (quickly driving the temperature of the Li-ion cell face coupled to the Peltier modules to the selected set point) was not really achieved. These results are discussed in the next subsection. Figure 4 shows a heating and a cooling experiments where the temperature of the Li-ion cell face with the Peltier modules was effectively controlled (quickly reaching the chosen set point and not drifting too away from it). Both tests were performed with the two Peltier modules connected in series to the switched power supply, each of them subjected to 6 V (but with the PWM acting to restrict the effective current in accordance with the control algorithm).

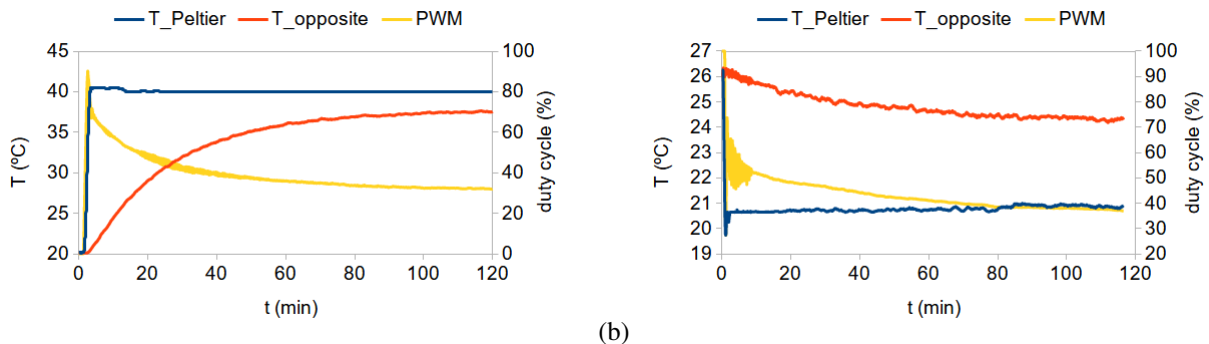


Figure 4. Results from experiments of cell heating (a) and cooling (b), where the temperature at the Peltier module side of the Li-ion cell was reasonably controlled.

The results of the heating test shown in Fig. 4(a) were considered satisfactory. The limited resolution of the temperature measurements is visible, but is not problematic. The results of the cooling test in Fig. 4(b), however, clearly show an excessive noise (even after smoothed by a moving average filter). Further tests revealed that this noise was essentially absent when the linear power supply was used instead of the (lighter and cheaper) switched power supply. Some switching, however, is inherent to the use of PWM, and seems to be recommendable the substitution of the analog temperature sensors used in the present work by digital sensors like the DS18B20 (Analog Devices, 2023) used by Cunha (2019), that are less susceptible to electromagnetic noise. A waterproof encapsulation (lacked by the LM35 used here) is also recommended for these sensors as air moisture condensation plagued the cooling tests.

3.2 The difficulties in cooling

As mentioned in the introduction, the cooling is expected to be more difficult than the heating. The difficulties found in trying to promote a twenty degrees step change in cooling (equivalent to that readily obtained in the heating test) were such that none of the attempts to be reported here was deemed well succeeded. Figure 5 shows the results of the sequence

of these attempts. The sequence begins in the Fig. 5(a) obtained using 6 V. Then comes Fig. 5(b) obtained using 8.5 V from the adjustable linear power supply. Figure 5(c) was obtained using 12 V and finally Fig. 5(d) was obtained using a second time 12 V but with a more powerful heat sink cooling the hot side of the Peltier modules.

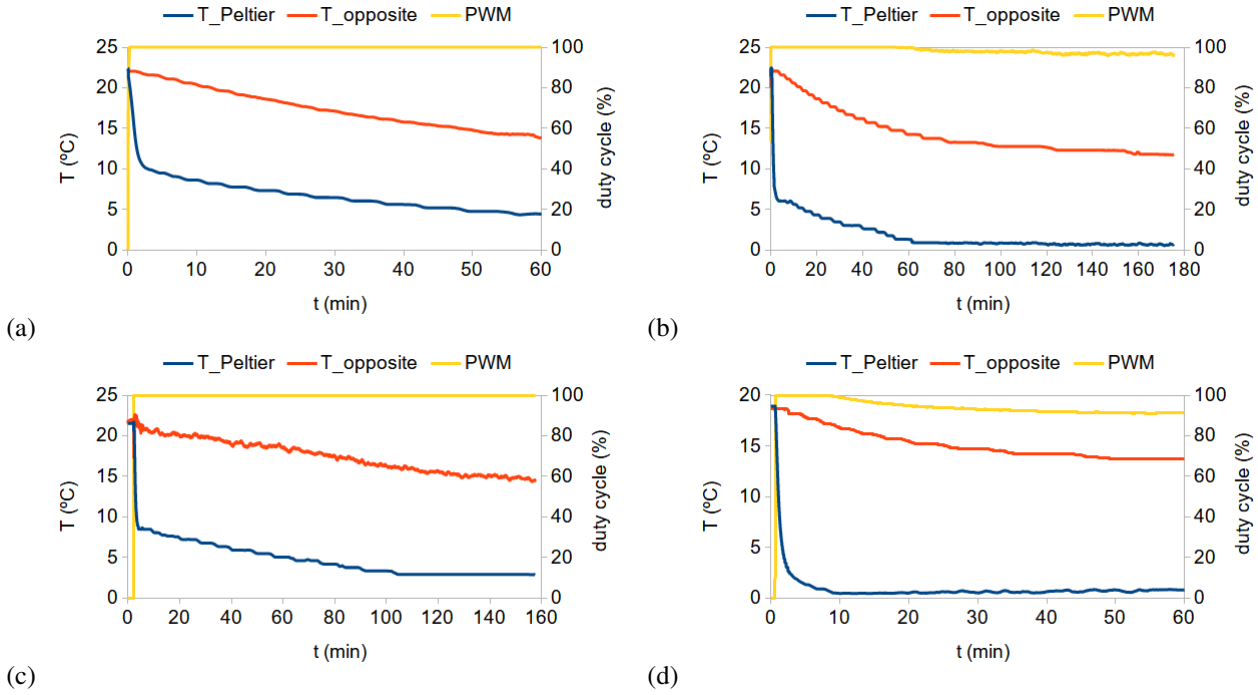


Figure 5. Results from experiments where the temperature at the Peltier module side of the Li-ion cell was reasonably controlled.

The results shown in the Fig. 5 illustrate the main aspect of the manufacturers performance maps (TE Technology, 2013): if the hot side of the Peltier module is adequately cooled, to increase the voltage increases the refrigeration capacity. If the voltage is increased without an adequate cooling of the hot side of the Peltier module, the refrigeration capacity falls. The more powerful heat sink used to obtain the improved refrigeration capacity revealed in the Fig. 5(d) is rather voluminous and hardly a good design option. Using a water block (that also facilitates an estimate of the heat removed by measuring the water flow and temperatures at its inlet and outlet) seems to be a much better option.

4. MATHEMATICAL MODEL

The experiments where the temperature control was effective (results shown in the section 3.1) can be reasonably modeled by the linear transient one-dimensional heat conduction differential equation shown below with the following initial and boundary conditions

$$\frac{\partial^2 \theta}{\partial x^2} = \frac{1}{\alpha} \frac{\partial \theta}{\partial t} \quad \theta \Big|_{t=0} = 0 \quad \theta \Big|_{x=0} = 1 \quad \left(\frac{\partial \theta}{\partial x} - \frac{U}{k} \theta \right) \Big|_{x=L} = 0 \quad (1)$$

where x and t are the spatial and temporal coordinates respectively,

$$\theta = \frac{T(x, t) - T_0}{T_P - T_0} \quad (2)$$

is the dimensionless temperature, with $T(x, t)$ being the primitive unknown temperature function, T_0 the initial temperature of the Li-ion cell, and T_P the temperature imposed by the Peltier modules at one of the largest cell faces. α is the cell thermal diffusivity (in the x direction, since prismatic Li-ion cells are usually modelled as orthotropic media). U is the global heat transfer coefficient between the opposite (to that with temperature controlled by the Peltier modules) cell largest face and the external environment. That environment is supposed to remain, throughout the experiment, at the same temperature T_0 at which the cell was at $t = 0$. k is the cell thermal conductivity (in the x direction) and α the corresponding thermal diffusivity.

The initial-boundary value problem denoted by Eq. (1) is a non-homogeneous one, but its solution may be obtained as the superposition, $\theta = \theta_s + \theta_h$, of the solution θ_s of a steady state non-homogeneous problem and the solution θ_h of an

homogeneous transient problem easily solved by separation of variables, as taught in textbooks (Öziçik, 1993). So

$$\theta = 1 - \frac{U}{k + UL} x - \sum_{m=1}^{\infty} c_m \exp(-\alpha \beta_m^2 t) \sin(\beta_m x) \quad (3)$$

where coefficients determined by the initial condition of the associated homogeneous problem are

$$c_m = \frac{1}{\beta_m N(\beta_m)} \left\{ 1 - \cos(\beta_m L) - \frac{U}{k + UL} \left[\frac{\sin(\beta_m L) - \beta_m L \cos(\beta_m L)}{\beta_m} \right] \right\} \quad (4)$$

the eigenvalues β_m are the roots of

$$k \beta_m \cot(\beta_m L) + U = 0 \quad (5)$$

and

$$N(\beta_m) = \frac{[\beta_m^2 + (U/k)^2] L + U/k}{2 [\beta_m^2 + (U/k)^2]} \quad (6)$$

are the norms of the eigenfunctions $\sin(\beta_m x)$.

4.1 Theoretical results compared with experiments

Table 1 shows most of the values used to obtain the theoretical results to be discussed here. The cell thickness and its density are easily measured in any cell. The specific heat appearing in the table was determined through the relatively unsafe calorimetric method mentioned in the introduction. One goal, now, is to use the experimental results, combined with the mathematical model, to verify the value of the cell thermal conductivity, that is expected to be near the value shown in the table, given by Kleiner *et al.* (2020) for a smaller cell from a different manufacturer, but also prismatic in shape and with NMC chemistry.

Table 1. Properties used to model the CALB L221N113A cell

Property	symbol	unit	value
Thickness	L	m	3.336×10^{-2}
Thermal conductivity ⁽¹⁾	k	W/(m·K)	0.7
Density	ρ	kg/m ³	2.3×10^3
Specific heat	c_p	J/(kg·K)	9.3×10^2

⁽¹⁾ Across the cell thickness (a larger value is observed in directions parallel to the largest faces).

Another variable to be estimated by comparing the experimental and theoretical results is the global coefficient of heat transfer U . It is interesting to note that these two variables, k and U appear in the model grouped: the global coefficient of heat transfer appears divided by the thermal conductivity and the thermal conductivity appears also grouped with the density and the specific heat in the thermal diffusivity formula

$$\alpha = \frac{k}{\rho c_p} \quad (7)$$

Recognizing, however, that once the density and specific heat are chosen, the thermal diffusivity is proportional to thermal conductivity and recalling that that the diffusivity is the property determining the speed of the temperature rise when the material is heated (or of the temperature fall when it is cooled) the possibility of tuning the thermal conductivity to make the model reproduce a temperature response time experimentally observed becomes clear. With the conductivity tuned it is easy to choose the global coefficient of heat transfer in such a way to match the steady state temperature found experimentally. Normally the estimation of both variables will take some iterations.

The procedure resumed in the preceding paragraph, that could be refined until become a parameter estimation inverse problem solution technique, is essentially what was done for confirming the thermal conductivity already given in Tab. 1 and estimate the global coefficient of heat transfer for the heating experiment as $U = 3$ W/(m²·K) and for the cooling experiment something around $U = 50$ W/(m²·K). These were the values used in calculating the theoretical and to nondimensionalize the experimental results depicted in the Fig. 6. To make Fig. 6 understandable, however, the definitions of the dimensionless time (Fourier number)

$$\tau = \frac{\alpha t}{L^2} \quad (8)$$

and of the dimensionless heat transfer coefficient (Biot number)

$$\text{Bi} = \frac{U L}{k} \quad (9)$$

used there, must be given

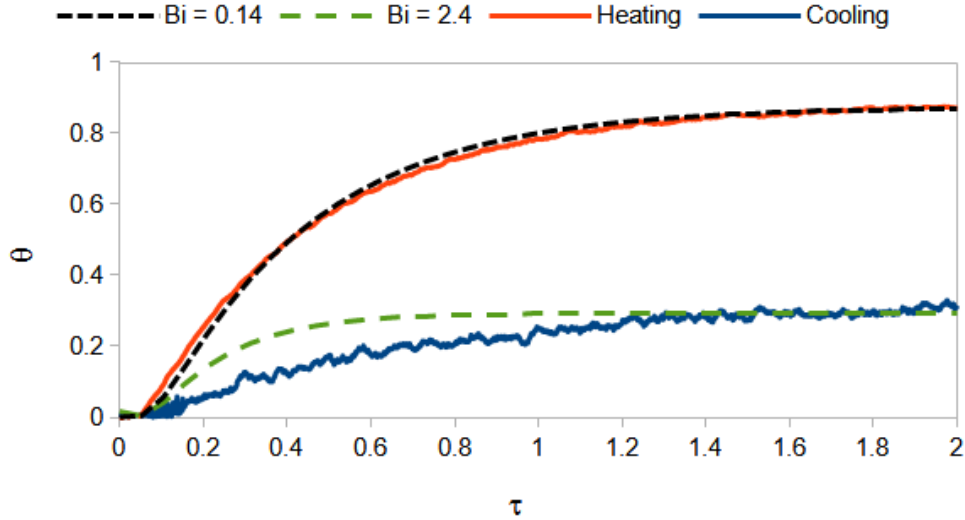


Figure 6. Comparison between experimental and theoretical dimensionless temperatures at the face opposite to that where the Peltier modules were placed.

Figure 6 seems to depict a good agreement between the experimental and theoretical temperatures when the Peltier module was used to heat the Li-ion cell. The $U = 3 \text{ W}/(\text{m}^2 \cdot \text{K})$ global coefficient of heat transfer used to obtain this agreement, however, is at least three times larger than what was expected. Considering just the $L_{\text{eps}} = 40 \text{ mm}$ thickness of insulation in expanded polystyrene with conductivity $k_{\text{eps}} \approx 0.038 \text{ W}/(\text{m} \cdot \text{K})$ one would get

$$U < \frac{k_{\text{eps}}}{L_{\text{eps}}} \approx \frac{0.038 \text{ W}/(\text{m} \cdot \text{K})}{0.040 \text{ m}} = 0.95 \text{ W}/(\text{m}^2 \cdot \text{K}) \quad (10)$$

Probably the non-uniformity of the temperature in the Li-ion cell face heated by the Peltier module lead the experimental heat flux field to important deviations from the uni-dimensional character hypothesized in the mathematical model. The global heat transfer coefficient is therefore overestimated to accommodate heat losses that, in reality, were not to the environment (through the polystyrene insulation) but to cell extremities inadequately heated by the Peltier module.

In the case of cooling the condensation make these deviations from uni-dimensional heat flux much larger. An aggravating aspect of this most well succeeded cooling experiment, with results shown in the Figs. 4(b) and 6, is that the temperature step chosen was four times smaller than the temperature step selected in the heating experiment. This choice was made to make the cooling easier to the Peltier modules (even without very efficient heat sinks coupled to their hot side) and minimize condensation. It led, however, to a proportionally small signal-to-noise ratio in the temperature response.

5. PROBLEMS AND RECOMMENDATIONS

The goals declared in subsection 1.1 were not fully accomplished yet, and the main findings of the present work are the problems to overcome. A list of these problems and solutions devised for them is presented below.

- Heat sinks: small water blocks can remove a higher heat rate than voluminous heat sinks that are more difficult to arrange spatially around a prismatic Li-ion cell. Additionally, the water blocks allow the estimation of the heat it removes by measuring the water temperature at its inlet and outlet.
- Small quantity of Peltier modules: as low cost Peltier modules do not have a high cooling capacity, to use more of them at the larger faces of the prismatic Li-ion cell is recommended. Besides improving the cooling or heating capacity the larger quantity of Peltier modules can render more homogeneous the temperature at the faces where they are applied.
- Analog temperature sensors: the use of digital temperature sensors, less susceptible to electromagnetic interference, avoids the high level of noise observed in analog temperature sensors signals when using compact switched power sources.

- Air humidity condensation: to deal with air humidity condensation in this kind of experiment adds difficulties at thermal insulation and risks to the integrity of the test equipment and of the Li-ion cell being tested. Therefore, avoid to cool down surfaces near the Li-ion cell to temperatures below the surrounding environment dew point is recommended.

Refrigerating in hot environments is almost always more challenging than heating in cold environments, as we expect from our knowledge of the Second Law of Thermodynamics. So, all the above problems are more acute, and some only exists, in the Li-ion cell cooling. Nonetheless, these recommendations should provide a good guidance to perfect the equipment being developed, before trying to couple it to an electronic load and a solution for the heat conduction with heat generation inside the prismatic Li-ion cell, to allow a more complete characterization of this kind of cell.

6. CONCLUSION

In the present work low cost Peltier modules were used to heat and to cool a Li-ion battery prismatic cell at one of its largest faces. The heating was performed with little difficulty, but to heat using electric resistances is easy and inexpensive, although less energetically efficient. The cooling possibility, that is the most appealing advantage of using Peltier modules, demanded much more work and was quite precariously realized. The difficulties in cooling were mostly related to the need of a really powerful heat sink effectively coupled to the hot side of the Peltier modules and also to the condensation that takes place when the temperature goes below the dew point of the surrounding air.

Notwithstanding these difficulties a comparison, between temperatures observed at the Li-ion cell largest surface opposed to that where the Peltier modules were coupled and those predicted by a simplified mathematical model, was possible. This comparison allowed an assessment of the Li-ion cell thermal conductivity, a coarse estimate of the heat transfer between the cell and the environment and brought a better insight on the experimental difficulties.

Developing a low cost equipment for heating and cooling Li-ion cells (without immersing them in water) is a worthy goal. It was not fully realized in the present work, but hopefully its realization will be helped by what was learnt in it. The mathematical model parameter estimation employing this equipment is also interesting and deserves further efforts. Nevertheless even more ambitious goals can be pursued, like evaluating the heat generated by the Li-ion cell when it is being charged or discharged with one of its faces at a fixed temperature (nowadays tests are performed with the temperature of the air surrounding the cell fixed, but the cell surfaces temperature vary according factors such as the air velocity field around the cell). To accomplish that, the experimental apparatus here described need not only to be improved, but also complemented by instruments enough to measure every bit of heat leaving (or getting into) the cell and to control the amperage (or voltage) of charge and discharge. The thermal part of the equipment that would result of such developments probably will end up being a kind of modernized guarded hot plate apparatus (ISO 8302) like HFM (2023), but hopefully cheaper. Overcoming the difficulties reported here, however, comes first.

7. ACKNOWLEDGEMENTS

The authors acknowledge the financial support from ANEEL, CELESC, EMBRAPII and IFSC. The authors are thankful also for the collaboration of many colleagues and students at IFSC and UFSC.

8. REFERENCES

- Analog Devices, 2023. "DS18B20 programmable resolution 1-wire digital thermometer". Available at Analog Devices, Inc. website. URL <https://www.analog.com/en/products/ds18b20.html#product-overview>.
- Beauregard, B., 2017. "Arduino PID library - version 1.2.1". Available in the Arduino IDE Library Manager and at GitHub. URL <https://github.com/br3ttb/Arduino-PID-Library>.
- Cunha, L.H.T., 2019. "Adaptive control applied to refrigeration systems using peltier modules (in Portuguese)". Control and Automation Engineering course completion work, Federal University of Minas Gerais. URL http://www.cpdee.ufmg.br/~victorcosta/pdfs/LudmilaCunha_Monografia_Final.pdf.
- Gonçalves, J.M., Abreu, S.L., Santos, L.A., Bresolin, A.A., Fuerback, A.L. and Costa, D.G., 2022. "Electrothermal simulation of electric vehicle battery under driving conditions". Proceedings of the 19th Brazilian Congress of Thermal Sciences and Engineering - ENCIT 2022. URL <https://www.sistema.abcm.org.br/articleFiles/download/36995>.
- Hermes, C.L. and Barbosa, J.R., 2012. "Thermodynamic comparison of peltier, stirling, and vapor compression portable coolers". *Applied Energy*, Vol. 91, No. 1, pp. 51–58. URL <https://www.sciencedirect.com/science/article/pii/S0306261911005538>.
- HFM, 2023. "HFM – Heat Flow Meter". Linseis GmbH. URL <https://www.linseis.com/en/products/thermal-conductivity-instruments/hfm-heat-flow-meter/>.
- ISO 8302, 1991. "Thermal insulation – Determination of steady-state thermal resistance and related properties – Guarded hot plate apparatus". Standard, International Organization for Standardization.

- Kleiner, J., Komsiyyscka, L., Elger, G. and Endisch, C., 2020. “Thermal modelling of a prismatic lithium-ion cell in a battery electric vehicle environment: Influences of the experimental validation setup”. *Energies*, Vol. 13, No. 1. URL <https://www.mdpi.com/1996-1073/13/1/62>.
- Li, X., Zhong, Z., Luo, J., Wang, Z., Yuan, W., Zhang, G., Yang, C. and Yang, C., 2019. “Experimental investigation on a thermoelectric cooler for thermal management of a lithium-ion battery module”. *International Journal of Photoenergy*, Vol. 2019, p. 3725364. URL <https://doi.org/10.1155/2019/3725364>.
- Liu, G. and Lijun, Z., 2021. “Research on the thermal characteristics of an 18650 lithium-ion battery based on an electrochemical–thermal flow coupling model”. *World Electric Vehicle Journal*, Vol. 12, p. 250. URL <https://doi.org/10.3390/wevj12040250>.
- Lyu, Y., Siddique, A.R.M., Gadsden, S.A. and Mahmud, S., 2021. “Experimental investigation of thermoelectric cooling for a new battery pack design in a copper holder”. *Results in Engineering*, Vol. 10, p. 100214. URL <https://doi.org/10.1016/j.rineng.2021.100214>.
- Maleki, H., Hallaj, S.A., Selman, J.R., Dinwiddie, R.B. and Wang, H., 1999. “Thermal properties of lithium-ion battery and components”. *Journal of The Electrochemical Society*, Vol. 146, p. 947. URL <https://doi.org/10.1149/1.1391704>.
- Mathworks, 2023. “Use of Peltier device as thermoelectric cooler”. Available at The MathWorks, Inc. website. URL <https://www.mathworks.com/help/sps/ug/use-of-peltier-device-as-thermoelectric-cooler.html>.
- Murashko, K., Pyrhönen, J. and Jokiniemi, J., 2020. “Determination of the through-plane thermal conductivity and specific heat capacity of a Li-ion cylindrical cell”. *International Journal of Heat and Mass Transfer*, Vol. 162, p. 120330. URL <https://doi.org/10.1016/j.ijheatmasstransfer.2020.120330>.
- Muratori, M., Canova, M., Guezennec, Y. and Rizzoni, G., 2010. “A reduced-order model for the thermal dynamics of Li-ion battery cells”. *IFAC Proceedings Volumes*, Vol. 43, pp. 192–197. URL <https://www.sciencedirect.com/science/article/pii/S1474667015368270>.
- Normey-Rico, J.E. and Morato, M.M., 2021. *Introduction to process control (in Portuguese)*. Editora Edgard Blücher Ltda., São Paulo.
- Santos, L.A., Gonçalves, J.M., Abreu, S.L., Costa, D.G., Fuerback, A.L. and Bresolin, A.A., 2022. “An initial study on an EV battery prismatic cell thermal behavior”. Proceedings of the 19th Brazilian Congress of Thermal Sciences and Engineering - ENCIT 2022. URL <https://www.sistema.abcm.org.br/articleFiles/download/36552>.
- Singh, H., Jain, N., Raj, S., Menon, V.U. and Herle, H., 2021. “Battery BTMS using Peltier cooler”. *International Research Journal of Engineering and Technology*, Vol. 8, pp. 4082–4086. URL <https://www.irjet.net/archives/V8/i6/IRJET-V8I6738.pdf>.
- TE Technology, 2013. “TE-127-1.4-1.5 thermoelectric module (Peltier module) specifications”. Available at TE Technology, Inc. website. URL <https://tetech.com/wp-content/uploads/2013/11/TE-127-1.4-1.5.pdf>.
- Thermoelectric Cooling, 2023. “Wikipedia”. Wikimedia Foundation. URL https://en.wikipedia.org/wiki/Thermoelectric_cooling.
- Öziçik, M.N., 1993. *Heat Conduction*. Wiley-Interscience, 2nd edition.

9. RESPONSIBILITY NOTICE

The authors are solely responsible for the printed material included in this paper.